Key role of glycoprotein Ib/V/IX and von Willebrand factor in platelet activation-dependent fibrin formation at low shear flow

*Judith M. E. M. Cosemans,[1] *Saskia E. M. Schols,[1,2] Lucia Stefanini,[3] Susanne de Witt,[1] Marion A. H. Feijge,[1] Karly Hamulyák,[2] Hans Deckmyn,[4] Wolfgang Bergmeier,[3] and Johan W. M. Heemskerk[1]

Departments of [1]Biochemistry and [2]Internal Medicine, Cardiovascular Research Institute Maastricht, Maastricht University and Maastricht University Medical Centre, Maastricht, The Netherlands; [3]Department of Medicine, Division of Hematology, and Cardeza Foundation for Hematologic Research, Thomas Jefferson University, Philadelphia, PA; and [4]Laboratory for Thrombosis Research, KU Leuven Campus Kortrijk, Kortrijk, Belgium

A microscopic method was developed to study the role of platelets in fibrin formation. Perfusion of adhered platelets with plasma under coagulating conditions at a low shear rate (250^{-1}) resulted in the assembly of a star-like fibrin network at the platelet surface. The focal fibrin formation on platelets was preceded by rises in cytosolic Ca^{2+}, morphologic changes, and phosphatidylserine exposure. Fibrin formation was slightly affected by $\alpha_{IIb}\beta_3$ blockage, but it was greatly delayed and reduced by the following: inhibition of thrombin or platelet activation; interference in the binding of von Willebrand factor (VWF) to glycoprotein Ib/V/IX (GpIb-V-IX); plasma or blood from patients with type 1 von Willebrand disease; and plasma from mice deficient in VWF or the extracellular domain of GpIbα. In this process, the GpIb-binding A1 domain of VWF was similarly effective as full-length VWF. Prestimulation of platelets enhanced the formation of fibrin, which was abrogated by blockage of phosphatidylserine. Together, these results show that, in the presence of thrombin and low shear flow, VWF-induced activation of GpIb-V-IX triggers platelet procoagulant activity and anchorage of a star-like fibrin network. This process can be relevant in hemostasis and the manifestation of von Willebrand disease. (*Blood*. 2011;117(2): 651-660)

Introduction

Platelets have prominent and divergent roles in the stimulation of blood coagulation. In vivo and in vitro evidence indicates that platelet-associated tissue factor triggers the extrinsic coagulation pathway.[1,2] In the presence of collagen, platelets contribute to the intrinsic, factor XII–dependent pathway of coagulation.[3,4] Furthermore, platelets stimulated by combinations of potent platelet agonists produce large amounts of thrombin because of exposure of phosphatidylserine (PS). This negatively charged phospholipid provides a surface on which the tenase and prothrombinase complexes assemble to produce factor Xa and thrombin, respectively.[5,6] Such platelets have been termed procoagulant or coated platelets; the latter designation refers to their property to assemble a protein coat consisting of granule-derived proteins, coagulation factors, fibrin(ogen), and von Willebrand factor (VWF).[7,8] Under static conditions, the procoagulant platelet response is suppressed by $\alpha_{IIb}\beta_3$ antagonists,[9,10] suggesting that this integrin has a regulating role in the coagulation process.

The glycoprotein Ib-V-IX (GpIb-V-IX) complex, expressed at more than 20 000 copies per platelet, can act as a ligand for VWF and various coagulation factors. Quantitative or qualitative abnormalities either in the GpIb-V-IX complex (in Bernard-Soulier syndrome) or in VWF (in von Willebrand disease [VWD]) are accompanied by impaired hemostasis and increased bleeding risk.[11,12] Although this points to a general role of GpIb-V-IX in platelet function, the signaling consequences of VWF–GpIb-V-IX interaction have mostly been studied under flow at high arterial shear rates.[11] However, there is limited evidence for a role of VWF and GpIb in the coagulation process in the absence of high-shear flow. It has been reported that VWF in the presence of fibrin stimulates GpIb-dependent thrombin generation under semistatic conditions.[13,14] In coagulation, VWF can have a carrier function for factor VIII (FVIII) and supply this factor to a growing thrombus.[15,16] Other authors propose a coagulation-stimulating role of GpIb by interaction with factor VIIa or thrombin[17,18] or a function of GpIb in fibrin binding to $\alpha_{IIb}\beta_3$, VWF, or thrombin.[19-21] Hence, the GpIb-V-IX complex seems to be a central component in the interaction of platelets with VWF, thrombin and the coagulation end-product, fibrin. However, it is unclear whether the GpIb-V-IX complex merely acts as an assembling component of these plasma factors or also has an active role in establishing activation of these factors.

In this paper, we describe a new role of platelets operating under low-shear flow conditions: the focal formation of fibrin fibers. We demonstrate that this process actively relies on VWF-GpIb-V-IX–mediated platelet stimulation in the presence of thrombin traces, and a subsequent local burst of thrombin generation. Furthermore, we do not find a major contribution in this process of $\alpha_{IIb}\beta_3$ activation or FVIII supply by VWF.

Submitted January 4, 2010; accepted October 13, 2010. Prepublished online as *Blood* First Edition paper, October 29, 2010; DOI 10.1182/blood-2010-01-262683.

*J.M.E.M.C. and S.E.M.S. contributed equally to this study.

The online version of this article contains a data supplement.

The publication costs of this article were defrayed in part by page charge payment. Therefore, and solely to indicate this fact, this article is hereby marked "advertisement" in accordance with 18 USC section 1734.

Methods

Materials

Apyrase, bovine serum albumin (BSA), and prostaglandin E_1 (PGE_1) were obtained from Sigma-Aldrich; corn trypsin inhibitor (CTI) from Haematologic Technologies; and VWF-deficient plasma from Affinity Biologicals. Ristocetin, recombinant human tissue factor (Innovin), and FVIII-deficient plasma came from Dade Behring; SFLLRN and the fluorogenic thrombin substrate, Z-GGR-AMC, from Bachem; and thrombin substrate S2238 from Chromogenics. Fluo-4 and Fura-2 acetoxymethyl ester; Oregon Green (OG) 488–labeled annexin A5; Alexa Fluor (AF)647-labeled annexin A5 and OG488- and AF546-labeled fibrinogen were from Invitrogen. Cathepsin G and H-Phe-Pro-Arg chloromethyl ketone (PPACK) were from Calbiochem, and *O*-sialoglycoprotein endopeptidase from Cedarlane Laboratories. Recombinant human VWF A1 domain was provided by Drs B. de Laat and P. G. de Groot (University Medical Center, Utrecht, The Netherlands).[22]

Monoclonal antibodies (mAbs) against the *N*-terminal$^{1\text{-}289}$ globular domain of GpIbα were generated, as described before.[23-25] The 2D2 mAb blocks the thrombin binding site of GpIb; 6B4 interferes with the shear-induced and ristocetin/botrocetin-induced binding of VWF to GpIb; 12G1 blocks only the shear-induced binding of VWF to GpIb; 2D4 is an isotope-matched control antibody. Anti-VWF mAb 418, blocking the interaction with FVIII, was provided by Dr P. Lenting (Inserm 770, Paris, France).[26] Rabbit anti–human VWF and control antibodies were from Dako; fluorescein isothiocyanate (FITC) anti-CD62P mAb was from Beckman Coulter; blocking anti–P-selectin mAb AK4 from BD PharMingen. Chimeric mAb, abciximab, directed against $\alpha_{IIb}\beta_3$ and $\alpha_v\beta_3$, was from Centocor; the nonpeptide $\alpha_{IIb}\beta_3$ antagonist, tirofiban, from Merck; fibrinogen γ-chain dodecapeptide, HHLGGAKQAGDV, interfering with a different fibrinogen-binding sequence on α_{IIb} than RGDS, was obtained from Anaspec.

Healthy participants and patients

Blood was taken from healthy volunteers and 2 patients with type 1 VWD. Subjects gave full informed consent, and had not taken medication interfering with coagulation or platelet function for at least 2 weeks. Patient plasmas contained 10%-12% of normal ristocetin cofactor activity, although tissue factor–induced thrombin generation was in the normal range.

Animals

Animal experiments were approved by the Thomas Jefferson University animal experimental committees. Transgenic IL4Rα/GpIbα mice[27] and mice homozygous for VWF deficiency[28] were generated as described, and bred against a C57Bl/6 genetic background. In the IL4Rα/GpIbα mice, most of the extracellular domain of GpIbα is replaced by the extracellular domain of the human interleukin-4 receptor α. Mice were provided by Drs J. Ware (University of Arkansas) and D. Wagner (Harvard Medical School, Boston, MA). Platelet surface glycoproteins were in the normal range. Plasmas from *VWF*$^{-/-}$ mice were devoid of VWF oligomers or multimers.

Blood collection and platelet preparation

Human blood was collected into 1/10 volume of 129mM trisodium citrate, and used to prepare platelet-rich plasma (PRP) and washed platelets.[4] Blood collection was approved by the Maastricht University Medical Ethical Committee. Where indicated, platelets in plasma were loaded with 8μM of Fluo-4 acetoxymethyl ester.[4] Washed platelets were resuspended at 100×10^9/L in Hepes buffer pH 7.45 (10mM Hepes, 136mM NaCl, 2.7mM KCl, 2mM $MgCl_2$, 0.1% glucose, and 0.1% bovine serum albumin [BSA]) containing apyrase (0.1 U/mL). If needed, platelets were pretreated with cathepsin G (400nM)[29] or *O*-sialoglycoprotein endopeptidase (0.1 mg/mL)[30] for 1 hour at 37°C, and washed again. Platelet count was determined with a thrombocounter (Coulter Electronics). Platelet-free pooled plasmas were prepared by differential centrifugation of citrate-anticoagulated blood from 6 to 10 healthy donors. Pooled plasmas were aliquoted and immediately snap-frozen at −80°C until use.

Blood from wild-type and knockout mice was drawn under anesthesia and collected into 1/10 volume of 129mM trisodium citrate.[31] Mouse PRP and washed platelets were prepared as before.[32] Purified platelets were resuspended at 100×10^9/L into Tyrode-Hepes buffer pH 7.45 (5mM Hepes, 136mM NaCl, 2.7mM KCl, 0.42mM NaH_2PO_4, 2mM $MgCl_2$, 0.1% glucose, and 0.1% BSA) with 0.1 U/mL apyrase. Citrate-anticoagulated platelet-free plasma from animals was obtained by differential centrifugation[33] and immediately snap-frozen. Where indicated, washed mouse platelets were pretreated with *O*-sialoglycoprotein endopeptidase (0.1 mg/mL) for 30 minutes at 37°C.[30]

Platelet analysis and activation in suspension

Expression of GpIb levels on platelets was determined by flow cytometry using FITC-labeled anti–human GpIbα mAb M1638 (Sanquin), or anti–mouse GpIbα M043 mAb (Emfret). Agonist-induced rises in $[Ca^{2+}]_i$ were measured as described.[4]

Microscopic measurement of fibrin formation under flow

Degreased, uncoated glass coverslips were placed into a transparent parallel-plate flow chamber (dimensions: 50 μm deep and 3 mm wide), mounted at the stage of an inverted fluorescence microscope (Diaphot 200; Nikon), and rinsed with Hepes buffer pH 7.45. Coverslips in a flow chamber were incubated for 10-15 minutes under stasis with a suspension of washed platelets (100×10^9/L). Remaining unbound platelets were removed by 5 minutes of perfusion with Hepes buffer pH 7.45 containing 1% BSA to prevent further platelet spreading. Coating time was adjusted to achieve adhesion of 22 ± 4 platelets per microscopic field of 95 × 95 μm. Adhered platelets were superfused with citrate-anticoagulated plasma and $CaCl_2$-containing medium at a calculated total shear rate of 250 s^{-1}. For the human system, 10 vol/vol of human plasma were coperfused with 1 vol/vol of 100mM Hepes, 75mM $CaCl_2$, and 37.5mM $MgCl_2$ (pH 7.45). For the mouse system, 3 vol/vol of mouse plasma were coperfused with 1 vol/vol of 136mM Hepes, 20mM $CaCl_2$ and 7mM $MgCl_2$ (pH 7.45). At 60 seconds after the start of fibrin formation (lag time recorded), coverslips were stained with labeled annexin A5 (0.5 μg/mL) and/or labeled fibrinogen (100 μg/mL). During flow, phase contrast and fluorescent images were recorded using a 100×/1.3 NA oil immersion objective and a sensitive electron multiplier (EM) CCD camera system (Hamamatsu Sciences). Images from mouse platelets were recorded as described.[31] Agonists or antagonists and fluorescent probes were added to the blood or plasma, as indicated. To measure rises in $[Ca^{2+}]_i$, platelets were loaded with Fluo-4 acetoxymethyl ester before adhesion.[4]

Confocal microscopy and image analysis

Dual color confocal images were recorded with a 60×/1.4 NA oil immersion objective and a BioRad/Zeiss laser scanning microscope system capable of electronic zooming.[34] Confocal overlays with differential interference contrast images were produced with a Leica SP5 multiphoton laser-scanning system. For quantification, bright-field and fluorescence images were analyzed from more than 8 arbitrarily chosen microscopic fields. Subtracted phase-contrast images were generated using Metamorph software Version 7.5.0.0 (MDS Analytical Technologies), and analyzed for changes in pixel intensity above background without any contrast enhancement.

Thrombin generation in plasma

Thrombin generation was measured in pooled human plasma by determining cleavage of fluorogenic Z-GGR-AMC, as before.[35] Coagulation was triggered with tissue factor (1pM) or kaolin (1.5 μg/mL) and $CaCl_2$ (16.6mM, no phospholipids added unless indicated). Thrombin was also measured in plasma samples (50 μL) taken at the outlet of the flow chamber, collected into stop buffer (50mM Tris, 175 mM NaCl and 10mM ethylenediaminetetraacetic acid [EDTA], pH 7.9).

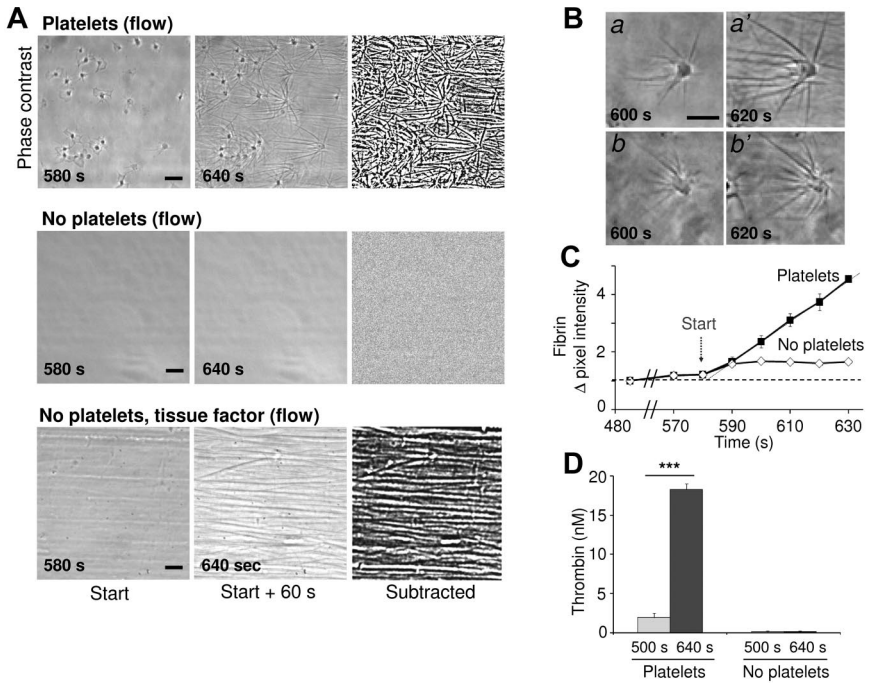

Figure 1. Platelet-dependent fibrin formation under flow. Coverslips with or without adhered platelets were perfused with pooled plasma under recalcification at a low shear rate of 250 s^{-1}. (A) Representative phase-contrast images taken at 580-640 seconds after start (ie, during the first minute of fibrin formation). Image recording with a Nikon Diaphot 200 microscope as described in "Methods." Right panels show differential, subtracted images (bars, 10 μm). Note the parallel fibrin fibers in the direction of flow on perfusion with tissue factor (1pM). (B) High magnification images of star-like fibrin fibers on platelets. (C) Quantification of fibrin fibers from subtracted images. Increases in mean pixel intensity are shown. (D) Thrombin activity in plasma samples collected from the flow chamber outlet. Means ± SE (n = 3-4 experiments); ***$P < .001$ vs control.

Statistics

The significance of differences was determined with the nonparametric Mann-Whitney U test and the paired sample *t* test (intervention effects), using the statistical package for social sciences (SPSS Version 11.0).

Results

Platelets promote star-like fibrin fiber formation under flow

A microscopic flow chamber method was developed to investigate the role of platelets in fibrin formation under flow conditions. Washed human platelets adhering to glass coverslips were perfused with plasma or blood that was recalcified to trigger coagulation. Coverslips were then blocked with Hepes buffer containing 1% BSA to prevent contact activation by the glass surface. Perfusion with normal pooled plasma at a low shear rate of 250 s^{-1} (but not at high shear rates) caused the sudden formation of star-like fibrin fibers on the majority of adhered platelets after a 10-minute lag time (Figure 1A). In control experiments with blocked coverslips not containing platelets, fibrin remained absent during more than 25 minutes, while tissue factor addition resulted in parallel fibrin fibers formed in the direction of flow (Figure 1A). With adhered platelets, inhibition of FVIIa (active-site inhibited FVIIa) or FXIIa (corn trypsin inhibitor) resulted in a 2-fold delay in star-like fibrin formation. This indicated that under these flow conditions both the intrinsic and extrinsic pathways contributed to overall coagulation process.

High-magnification microscopic images demonstrated a steadily growth in length of the fibrin fibers produced on platelets (Figure 1B; supplemental Video, available on the *Blood* Web site; see the Supplemental Materials link at the top of the online article). From subtraction images, the increase in fiber length was calculated at ~ 1 μm/s (supplemental Figure 1A-B), while the onset of fibrin formation was determined at ~ 580 seconds (Figure 1C). Plasma samples taken at the outlet of the flow chamber showed the presence of substantial amounts of thrombin, but only if platelets were present (Figure 1D). Under stasis, importantly, plasma recalcification did not result in measurable thrombin generation, unless tissue factor (lag time, 10 minutes) or kaolin (lag time, 19 minutes) was added (supplemental Figure 1C). Hence, in the flow experiments, the adhered platelets strongly promote the generation of thrombin and subsequent fibrin formation.

Activation of platelets is required for star-like fibrin formation

Bright-field and fluorescence microscopic images were recorded to determine the activation state of adhered platelets during perfusion with plasma. Before fibrin formation, most platelets displayed pseudopods (type 1) or lamellipods (type 2) while retaining a thick core. This indicated normal spreading over the surface. During flow, most of the cells changed into translucent structures with ruffled edges and a lost core (type 3), or into round, blebbing cells (type 4; Figure 2A). The type 3 and 4 structures resemble the description of cells with Sustained Ca^{2+} Induced Platelet (SCIP) morphology.[8,36] Platelet activation was confirmed by staining with OG488–annexin A5, showing PS exposure of most type 3/4 cells (Figure 2B). Labeling of annexin A5 was detectable after ~ 4 minutes of plasma perfusion, that is, before the appearance of fibrin (Figure 2C). Adhering Fluo-4–loaded platelets showed potent rises in cytosolic Ca^{2+} starting after ~ 3 minutes of perfusion (Figure 2D). Finally, after 12 minutes, 89% of the platelets showed exposed PS, while 96% showed fibrin stars (Table 1). In the presence of thrombin inhibitor PPACK, Ca^{2+} responses as well as PS exposure and fibrin formation were almost abolished.

Labeling with OG488-fibrinogen confirmed the star-like appearance of the fibrin fibers produced on platelets (supplemental Figure 2A). Colabeling with AF546-VWF indicated ~ 50% pixel-by-pixel overlap with OG488-fibrin(ogen), which is in agreement with the known ability of VWF to bind fibrin (supplemental Figure 2D). Labeled OG488-factor Xa gradually accumulated at the platelet

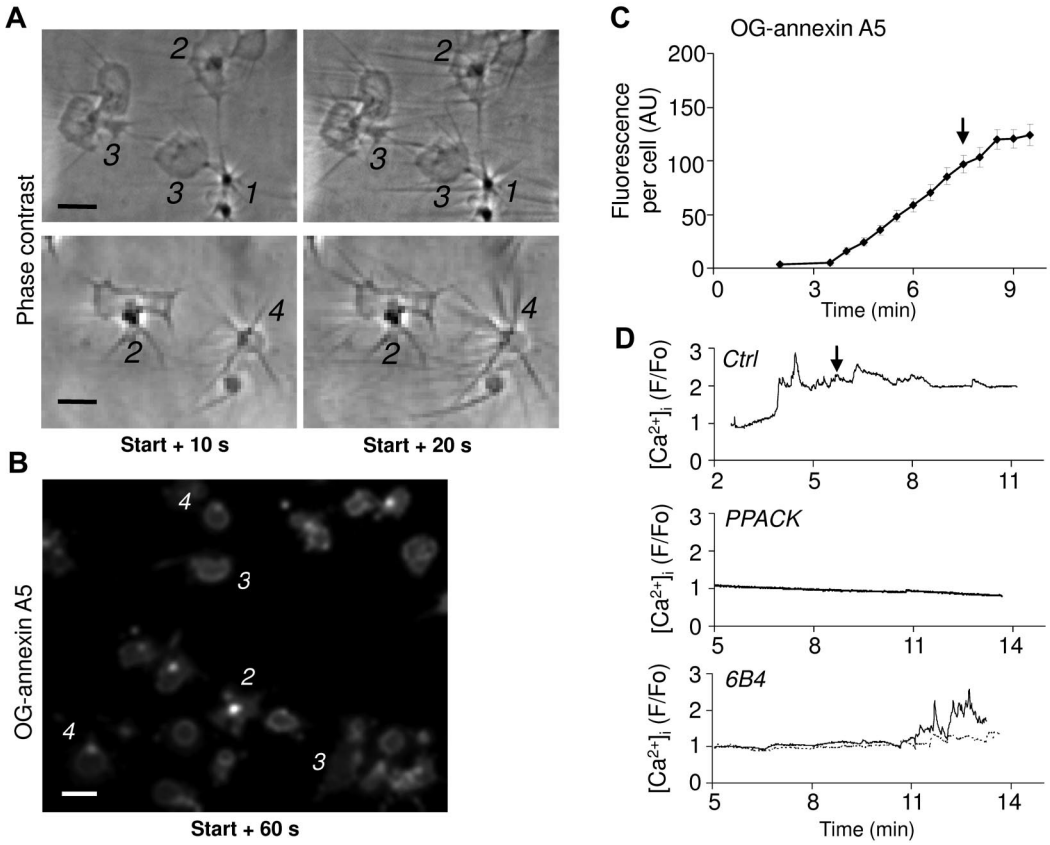

Figure 2. Morphologic activation score of fibrin-forming platelets. (A), Different morphologies of adhered platelets superfused with normal plasma at low shear rate of 250 s^{-1}. Start of fibrin formation was at 580 seconds. Numbers in italic refer to platelets with different structures: 1, platelet with pseudopods and core; 2, platelet with lamellipods and core; 3, translucent platelet without core, forming ruffled edges; 4, bleb-forming platelet with rounded structure (bars, 10 μm). (B), Fluorescence images after postlabeling with OG488–annexin A5. (C), Time-dependent increase in OG488–annexin A5 fluorescence during plasma perfusion (arbitrary fluorescence units per cell, mean ± SE, n = 12). Arrow points to start of fibrin formation. (D), Representative $[Ca^{2+}]_i$ rises of single adhered platelets during plasma perfusion, expressed as pseudo-ratio F/F_o values. Where indicated, PPACK (40μM) or 6B4 mAb (20 μg/mL) was present in plasma. Microscopic images and Ca^{2+} traces recorded with a Nikon Diaphot 200 microscope as described in "Methods."

surface, indicating factor Xa-dependent prothrombinase activity (supplemental Figure 2C). Although fibrin-forming platelets exposed P-selectin (supplemental Figure 2B), the blocking anti–P-selectin mAb AK4 (20 μg/mL) did not affect the lag time to fibrin formation (93% ± 7% of control) nor the appearance of the fibers.

To determine whether platelet activation is required for fibrin formation, adhered cells were treated with PGE_1, causing elevation in Cyclic adenosine monophosphate (cAMP), before perfusion with plasma. This treatment significantly increased the lag time to start of fibrin formation from 9.3 ± 0.5 minutes to 12.7 ± 1.4 minutes ($P < .05$; n = 4). Few of the PGE_1-treated platelets formed fibrin fibers and no longer had a star-like appearance (Figure 3A). Treatment with PGE_1 led to a marked reduction in the increase of Ca^{2+} and to diminished staining with labeled annexin A5 and fibrinogen (Figure 3B-D).

A thrombin receptor role was studied by platelet pretreatment with the protease cathepsin G, which cleaves PAR isoforms as well as GpIbα from the cell surface.[37-39] Control experiments confirmed

Table 1. Effect of various treatments on platelet activation and fibrin formation under flow

Treatment	Fraction of adhered platelets		
	Types 3 and 4	PS-exposing	Fibrin-forming
Initial (0 min)			
Control	0.12 ± 0.07	0.06 ± 0.03	0
After perfusion (12 min)			
Control	0.79 ± 0.04	0.89 ± 0.02	0.96 ± 0.04
PPACK	0.14 ± 0.04*	0.10 ± 0.05*	0
Cathepsin G	0.10 ± 0.03*	0.16 ± 0.09*	0.02 ± 0.01*
Annexin A5	0.08 ± 0.01*	N.d.	0.01 ± 0.01*

Adhered platelets were superfused with recalcified plasma at 250 $seconds^{-1}$, as described in Figure 1. Plasma was incubated with PPACK (40μM) or unlabeled annexin A5 (20 μg/mL), as indicated. Alternatively, platelets were pretreated with cathepsin G (400nM). After 0-12 minutes of perfusion, adhered platelets were classified as types 1-4 (pseudopods, lamellipods plus core, translucent without core, and bleb-forming, respectively) from phase-contrast images. Adhered platelets were counted as PS-exposing (staining with OG488-annexin A5) and forming fibrin fibers. Values reported are means ± SE (n = 3-6 experiments).

N.d. indicates not determined.

*$P < .01$ compared with control.

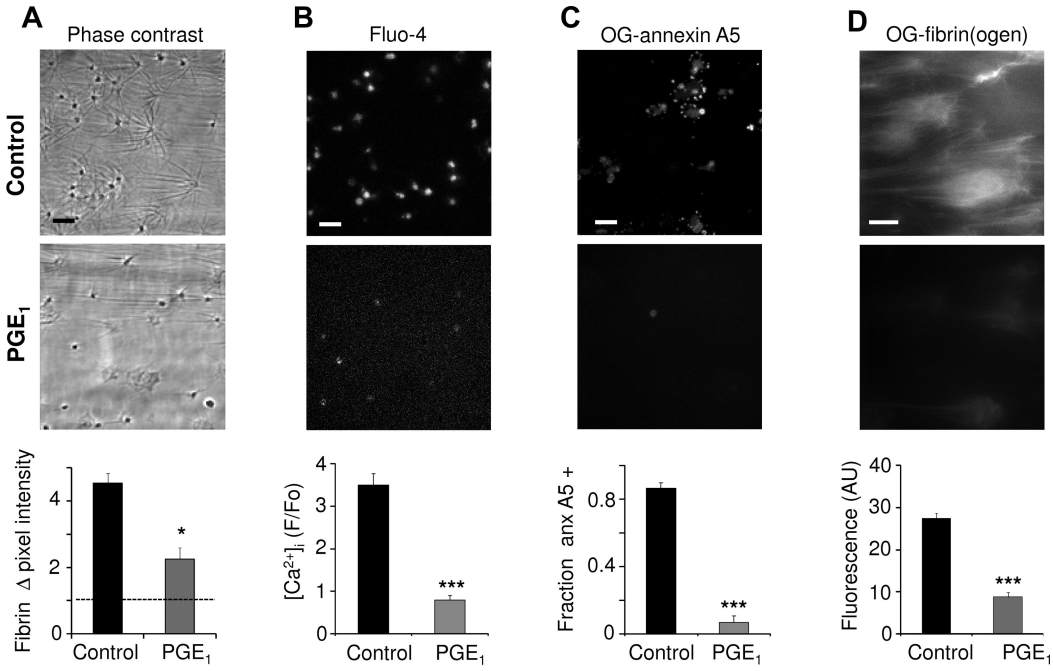

Figure 3. Effects of PGE_1 on platelet activation and fibrin formation. Platelets were superfused with plasma at 250 s^{-1} in the absence (control) or presence (0.5μM) of PGE_1. Bright-field and contrast images (Nikon Diaphot 200 microscope, see "Methods") were taken at 0-60 seconds after start of fibrin formation (bars, 10 μm). (A) Reduced fibrin on platelets after PGE_1 treatment (average pixel intensities of subtracted images). (B) Lower $[Ca^{2+}]_i$ rises with PGE_1 in Fluo-4–loaded platelets. (C) Lower OG488–annexin A5 staining with PGE_1. (D) Reduced OG488-fibrin(ogen) staining (integrated fluorescent intensities). Means ± SE; n ≥ 3; $^*P < .05$, $^{***}P < .001$ vs control.

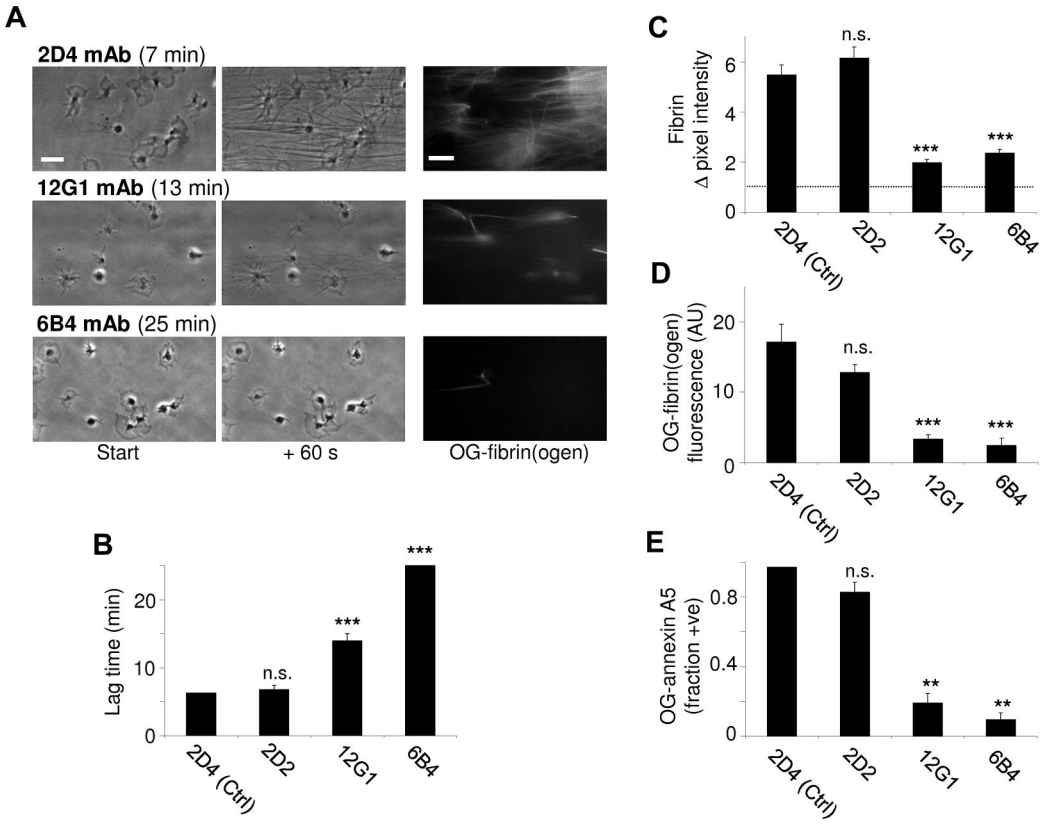

Figure 4. Role of platelet GpIb-V-IX in fibrin formation under flow. Platelets were superfused with plasma at 250 s^{-1} in the presence (10 μg/mL) of isotype control mAb 2D4 or one of the following anti-GpIbα mAbs: 2D2 (block of thrombin binding site), 12G1 (block of shear-induced VWF binding) or 6B4 (block of shear- and ristocetin-induced VWF binding). (A) Representative microscopic images (Nikon Diaphot 200 microscope, see "Methods") were taken at 0-60 seconds after start of fibrin formation: phase contrast and OG488-fibrin(ogen) (bars, 10 micron). (B) Lag time to start of fibrin formation. (C) Quantification of fibrin formation from subtracted images (60 seconds). (D) Staining with OG488-fibrin(ogen). (E) Fractions of platelets positive for OG488–annexin A5. Means ± SE; n = 3-4; $^{***}P < .001$ vs control mAb.

that the cathepsin G treatment greatly reduced thrombin-induced Ca^{2+} mobilization and GpIbα surface expression (supplemental Figure 3A-B). The treated platelets adhered normally, but, on perfusion with plasma, only 10%-16% developed a type 3/4 morphology and exposed PS, while no fibrin was formed (Table 1). Perfusion of untreated platelets in the presence of 20 μg/mL annexin A5, which blocks procoagulant cell membranes,[35] also abolished fibrin formation (Table 1). On the other hand, platelet treatment with the PAR-1 agonist SFLLRN was without effect (not shown). Together, these data showed the need of prior platelet activation and PS exposure for star-like fibrin formation.

Role of GpIb-V-IX but not $\alpha_{IIb}\beta_3$ in platelet fibrin formation

A possible role of integrin $\alpha_{IIb}\beta_3$ was then studied. Adhered platelets were perfused with plasma containing one of the following $\alpha_{IIb}\beta_3$ blockers: the chimeric mAb abciximab (20 μg/mL); the nonpeptide inhibitor tirofiban (5 μg/mL); or dodecapeptide derived from the fibrinogen γ-chain (200μM), which blocks a unique epitope on the α_{IIb} chain. Surprisingly, these integrin blockers only slightly affected the time to fibrin formation on platelets or fibrin growth (supplemental Figure 4).

A contribution of the GpIb-V-IX complex was studied by using a panel of mAbs (10 μg/mL) against different epitopes of the extracellular domain of GpIbα. The 2D2 mAb directed against the thrombin binding site on GpIbα influenced neither the lag time nor the extent of fibrin formation, in comparison to control mAb 2D4 (Figure 4A-B). On the other hand, the blocking mAbs 12G1 and 6B4, which are both directed against the VWF binding site on GpIbα, provoked marked prolongation of the lag time, accompanied by a major reduction in the amount of fibrin formed during 1 minute (Figure 4C-D). Most platelets retained their type 2 morphology, and no fibrin was formed during 25 minutes. The 6B4 mAb also markedly prolonged and reduced the Ca^{2+} responses (Figure 2D), while both mAbs abrogated PS exposure (Figure 4E). These results suggest a role of the VWF-binding domain of GpIb in platelet activation and subsequent fibrin formation.

Role of VWF-GpIb interaction in platelet fibrin formation

We studied a possible role of VWF in the formation of fibrin by knowing the partial colocalization of platelet-bound GpIbα ligand VWF with fibrin. First, normal plasma was incubated with ristocetin to stimulate the interaction of VWF with platelet GpIb. The ristocetin incubation significantly shortened the lag time to fibrin formation, while the amount of fibrin formed was unchanged (Figure 5A-B). Second, plasma was used from 2 patients with type 1 VWD (both with 10%-12% of normal ristocetin cofactor activity). With either plasma, fibrin formation on adhered platelets was significantly delayed and diminished in comparison to control plasma (Figure 5). In addition, the fractions of PS-exposing platelets were reduced from 76% to 19% ± 3% (control vs patient plasmas). Ristocetin treatment of patient plasmas did not alter the lag time or the extent of fibrin formation.

The importance of the GpIb-V-IX–VWF axis for fibrin formation was also studied in the mouse. Similar to the human system, low-shear flow of recalcified wild-type mouse plasma resulted in star-like formation of fibrin fibers on 80% of adhered platelets after a 12-minutes lag time. In marked contrast, essentially no fibrin formed up to 25 minutes, when using platelets and plasma from mice lacking the extracellular domain of GpIbα or from mice with VWF deficiency (Figure 6A-B). To further confirm the importance of GpIb, wild-type platelets were treated with O-sialoglycoprotein

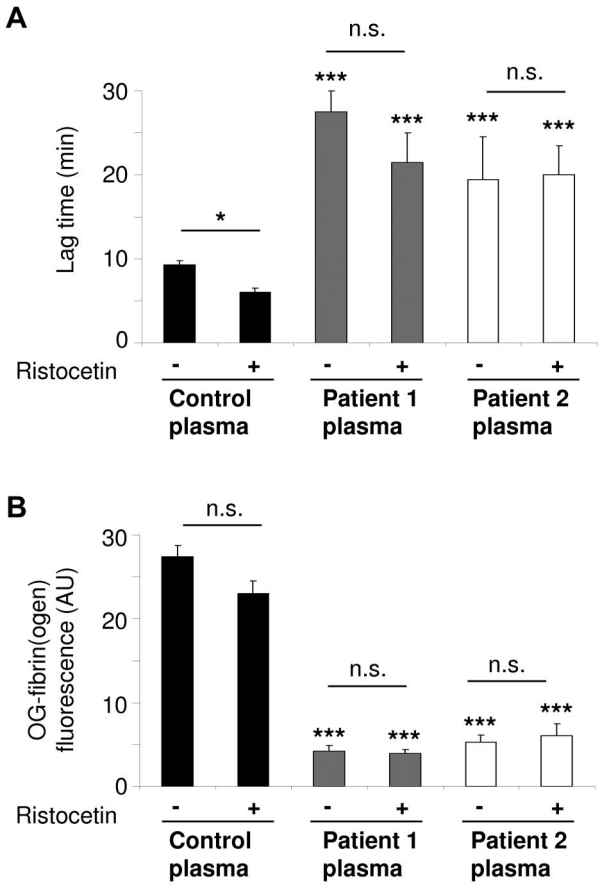

Figure 5. Role of plasma VWF in platelet fibrin formation under flow. Platelets were superfused with pooled plasma from control subjects (control) or from 2 patients with VWD at shear rate of 250 s^{-1}. Ristocetin (37.5 μg/mL) was added as indicated. Microscopic images were taken at start and after 60 seconds of fibrin formation. (A) Lag time to start of fibrin formation. (B) Quantification of OG488-fibrin(ogen) binding. Means ± SE; n = 3-4; $^*P < .05$, $^{***}P < .001$ vs control plasma.

endopeptidase, which cleaves off the 45 kD N-terminal region of mouse GpIbα.[40] This treatment resulted in > 95% loss of the surface expression of GpIbα (supplemental Figure 3C). On plasma perfusion, only 3% ± 3% of adhered endopeptidase-treated platelets bound annexin A5 (compared with 72% of untreated platelets), while the lag time to fibrin formation was lengthened to more than 25 minutes. Together, these results demonstrated a key role of VWF and GpIb in platelet activation and fibrin formation in the mouse system as well.

In subsequent experiments, adhered human platelets were prestimulated with ionomycin to provoke exposure of PS (Figure 7A-B). On perfusion, this greatly shortened the lag time to fibrin formation from 9.3 ± 0.5 minutes to 4.3 ± 0.8 minutes (Figure 7C-D). In this case, VWD plasma was similarly effective as control plasma. Notably, however, the anti-GpIb 6B4 mAb prolonged this lag time again to 8.3 ± 0.7 minutes, still pointing to a role of the GpIb-V-IX complex in fibrin fiber assembly.

Because FVIII in plasma is bound to VWF,[15] a possible role of VWF was investigated as local supplier of FVIII to the platelets. As expected, FVIII was required for coagulation, as perfusion with FVIII-deficient plasma did not result in fibrin formation on platelets. Reconstitution of this plasma with recombinant FVIII (Kogenate; Bayer) restored the time to fibrin formation from more than 20 minutes to 6.3 ± 1.3 minutes. Control plasma was then incubated with the anti-VWF mAb 418 (40 μg/mL), which displaces FVIII from VWF.[26] This mAb did not increase, but

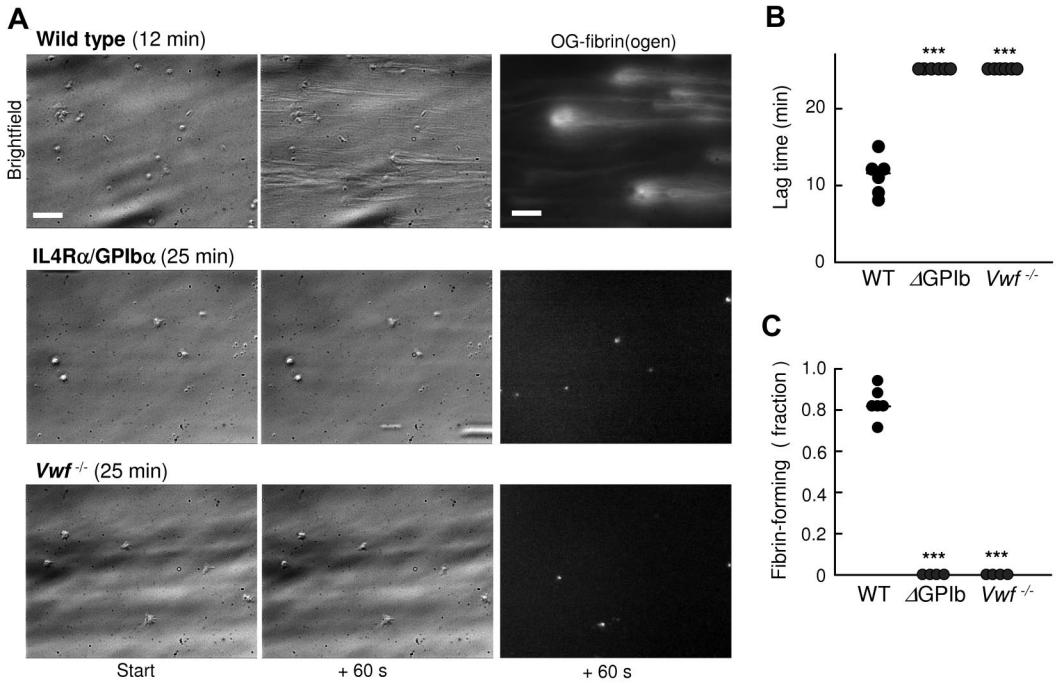

Figure 6. Roles of murine GpIb-V-IX and VWF on platelet-dependent fibrin formation under flow. Adhered platelets from wild-type (WT) mice, transgenic mice lacking the extracellular domain of GpIbα (IL4Rα/GpIbα), or mice deficient in VWF were superfused with autologous plasma at a shear rate of 250 s^{-1}. (A) Representative bright-field images (bars, 20 μm) after 0-60 seconds of fibrin formation, as well as images of OG488-fibrin(ogen). Images were recorded as described.[31] (B) Lag time to start of fibrin formation. (C) Fractions of fibrin-forming platelets during 25 minutes perfusion. Means ± SE; n = 4-6 mice; ***$P < .001$ vs WT.

insignificantly reduced the time to fibrin formation from 9.7 ± 1.4 to 7.0 ± 1.0 minutes ($P = .18$). As an alternative approach, the effect of recombinant VWF A1 domain was tested, which represents the GpIb–binding domain of VWF and does not interact with FVIII.[22] Reconstitution of VWF-deficient plasma with FVIII (Kogenate, 1 U/mL) decreased the time to fibrin formation on platelets from > 25 minutes to 15.1 ± 3.4 minutes ($P < .05$). Markedly, coaddition of A1 domain (5 μg/mL) further accelerated the fibrin formation to 7.5 ± 1.8 minutes, that is, similar to full-size VWF. Hence, the binding of VWF A1 domain to GpIb-V-IX appears to be sufficient for triggering fibrin formation on platelets, while a role of VWF-FVIII binding was not detectable.

Role of fibrin formation via GpIb-V-IX and VWF in flowing whole blood

To study the fibrin formation on platelets under physiologically relevant conditions, experiments were performed using recalcified whole blood. High-shear perfusion of blood over adhered platelets did not result in fibrin or thrombus formation. By stepwise lowering of the flow rate, star-like fibrin fibers on platelets appeared at a shear rate of 125 s^{-1} (Figure 8A). The fibrin formation was accompanied by deposition of platelets from the blood and thrombus formation. During low-shear flow, fluorescence from AF647–annexin A5 and AF547-fibrinogen was recorded in real time by dual color confocal microscopy. A gradual accumulation was observed of annexin A5 fluorescence (PS exposure), which within 20 seconds was followed by the appearance of AF547-fibrin fibers (Figure 8A-B). Both PS exposure and fibrin formation were delayed and diminished with VWD blood or with control blood containing the 12G1 anti-GpIb mAb. Furthermore, high-resolution images confirmed that also in whole blood PS-exposing platelets served as focal points for star-like fibrin formation (Figure 8C). In sum, these results point to a role of GpIb-V-IX and VWF in fibrin formation on platelets also in whole blood flowed at low shear rate.

Discussion

This article describes a new function of platelets operating under low-shear flow conditions to propagate the formation of star-like fibrin fibers at their surface. Mechanistically, this process relies on platelet activation evoked by VWF binding to GpIb-V-IX in the presence of traces of thrombin. The evidence comes from experiments showing that the fibrin formation on platelets in the presence of flow and coagulation is enhanced by ristocetin, antagonized by antibodies blocking the shear-dependent interaction of GpIbα with full-size VWF or VWF A1 domain, impaired in plasma or blood from VWD patients, greatly delayed in blood from mice deficient in VWF or the extracellular domain of GpIbα, and no more than slightly affected by integrin $\alpha_{IIb}\beta_3$ inhibition.

The time-dependent measurements show that during flow with plasma, adhered platelets assume an activated state (elevated Ca^{2+}, type 3/4 morphology, PS exposure, factor Xa binding) before the start of fibrin formation. This activation is nearly abolished in the presence of PPACK, thus pointing to role of in situ formed thrombin as coagonist. In addition, platelet inhibition with PGE_1 abrogates platelet Ca^{2+} rises and PS exposure, again accompanied by a delay and reduction in fibrin formation. This points to a scenario where the immobilized platelets respond to small amounts of thrombin in flowing plasma, which enforces VWF- and GpIb-mediated signaling to result in full platelet activation. Via a local enforcement loop, platelet-exposed PS activates coagulation factor complexes, which then generate sufficiently high thrombin amounts to ensure the focal fibrin formation. The importance of flow and

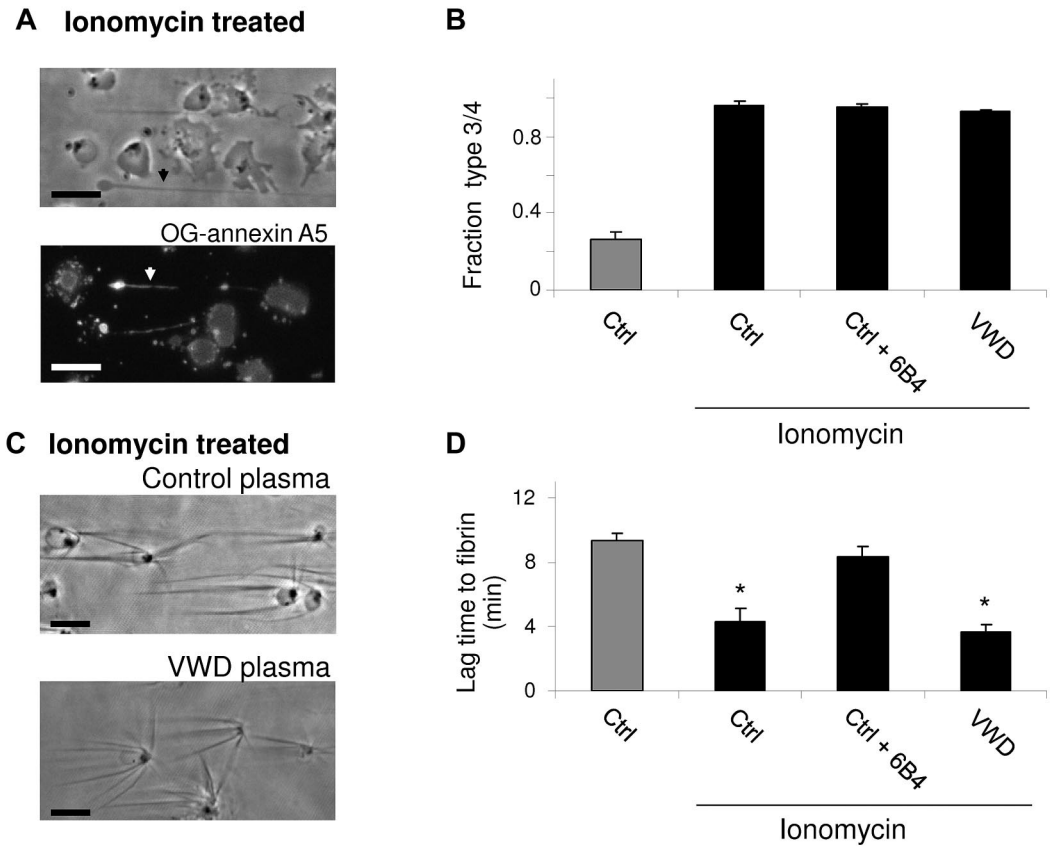

Figure 7. Rapid fibrin formation on ionomycin-stimulated platelets. Adhered platelets were prestimulated with ionomycin (10μM) and $CaCl_2$ (1mM), then perfused with control plasma (Ctrl) or plasma from a patient with VWD in the presence or absence of 6B4 mAb (10 μg/mL). (A) Representative phase contrast and OG–annexin A5 fluorescence images (Nikon Diaphot 200 microscope, see "Methods") after ionomycin stimulation (bars, 10 μm). (B) Fractions of type 3 and 4 (procoagulant) platelets before plasma perfusion. (C) Platelet-dependent fibrin formation after 240 seconds. (D) Lag time to fibrin formation after plasma perfusion. Means ± SE; n = 3-4.

GpIb in this process, in synergy with thrombin, is clearly demonstrated by the delayed and reduced platelet Ca^{2+} rises, PS exposure, and fibrin formation with blocking anti-GpIb mAbs 6B4 and 12G1, which specifically recognize an VWF-binding epitope on GpIbα that is exposed by shear or ristocetin/botrocetin-induced activation.[23] Similarly, GpIbα cleavage (by cathepsin G or O-sialoglycoprotein endopeptidase), GpIbα absence, or paucity in VWF (VWD patients and deficient mice) greatly impairs platelet PS exposure along with fibrin formation. A specific role of VWF as carrier for FVIII in (thrombin and) fibrin formation is not detected. This proposal is further supported by the finding that platelet preactivation with ionomycin, causing immediate PS exposure, enhances fibrin formation. However, blockage of GpIb still delays this process, indicating a role of GpIb independent of platelet activation.

The present recognition of VWF- and GpIb-mediated PS exposure and fibrin formation sheds a new light on several earlier findings. It is compatible with the known ability of GpIb-V-IX to provide a binding site for coagulation factors, VWF and, via VWF, for fibrin.[17,24,41,42] While other authors have shown that platelets can adhere to fibrin via GpIb,[18,20,42] the present data indicate that this binding also provides a means for attachment of growing fibrin fibers at the platelet surface. Our data confirm a role of GpIb-V-IX in thrombin generation,[13,17] but they also show that at least under flow this role is independent of preformed fibrin, $\alpha_{IIb}\beta_3$ activation or thrombin binding to GpIb. Furthermore, VWF appears to be important not only for stimulating platelet procoagulant activity, but also for focal fibrin formation.

The importance of VWF-induced platelet activation via GpIb has extensively been documented at high-shear flow conditions, provoking shear-dependent conformational changes in VWF and GpIb.[43,44] Interestingly, we find that, in the presence of low shear rate ($250\ s^{-1}$) and in situ formed thrombin, blocking of the shear/ristocetin-induced binding of VWF to GpIbα (6B4, 12G1 mAbs) effectively reduces platelet activation and fibrin formation. On the other hand, blocking of the thrombin binding site on GpIbα (2D2 mAb) is not effective. This points to a previously unrecognized VWF-induced GpIb-activating effect probably dependent on the presence of thrombin that results in platelet procoagulant activity and operates at low shear conditions. This might indicate that, under coagulant conditions with (traces of) thrombin present, a low shear rate can cause similar conformational changes, facilitating VWF interaction with GpIbα and platelet activation, as was previously reported for high shear rates. The relevance of these findings comes from animal studies demonstrating that deficiency in GpIbα or VWF affects not only arterial but also venous thrombus formation.[45,46] This indeed suggests a prothrombotic function of both proteins also at low, venous shear flow conditions.

Plasma perfusion carried out in the presence of corn trypsin inhibitor or inactivated factor VIIa show a twofold prolongation of the time to fibrin formation. The contribution of factor XII relies on the presence of adhered platelets because, under flow, no fibrin is formed without platelets. An interesting explanation is that platelets in some way trigger the contact activation system, eg by producing polyphosphates, which have been demonstrated to activate factor

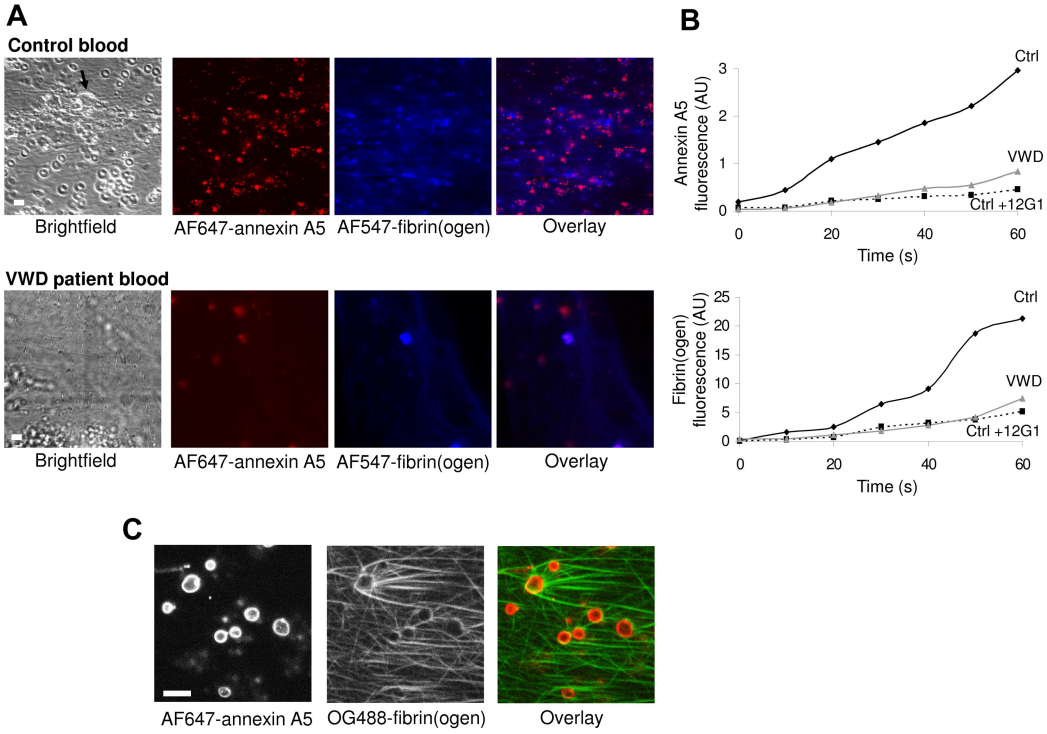

Figure 8. Contribution of GpIb-V-IX and VWF to fibrin formation in whole blood. Platelets were superfused with recalcified whole blood at a shear rate of 250 s^{-1} for 5 minutes, after which the flow was stepwise reduced every 2.5 minutes to reach 125 s^{-1} at 10 minutes. Blood from healthy control subjects (Ctrl) or type 1 VWD patients was supplemented with labeled fibrinogen (150 μg/mL), AF647–annexin A5 (0.5 μg/mL) and/or 12G1 mAb (10 μg/mL). Bright-field and confocal fluorescence images were captured at 10 minutes (t = 0) with a Biorad/Zeiss laser-scanning microscope system (see "Methods"). (A) Representative images taken after 60 seconds, showing clusters of PS-exposing platelets and a growing fibrin network. Arrow indicates thrombus (bars, 10 μm). (B), Time plots showing fluorescence accumulation of AF546-fibrin(ogen) (blue) and AF647–annexin A5 (red). (C), High-resolution confocal images of OG488-fibrin(ogen) and AF647–annexin A5 fluorescence. Data are representative of 3 or more experiments.

XII.[47] The result may be enhanced thrombin generation, and thereby fibrin generation. Further studies will resolve this issue.

The studies performed with mouse plasma and platelets provide some insight into the GpIb activation mechanism, because adhered platelets expressing the chimeric IL4Rα/GpIbα, lacking the extracellular domain of GpIbα, are unable to support fibrin formation, in spite of the fact that the intracellular domain of the glycoprotein normally interacts with filamin-1 and 14-3-3ζ.[27] Hence, other activation pathways play a role, probably involving protein tyrosine kinases.[48] Given the present data, the severe bleeding phenotype retained in these mice may be linked to defective platelet activation and fibrin formation. Similarly, in humans, this mechanism of platelet-dependent fibrin formation at low shear rate can be relevant for normal hemostasis, and may contribute to the bleeding risk seen in patients with deficiencies in VWF or GpIb-V-IX complex.

Acknowledgments

We thank Drs B. de Laat and P. G. de Groot for the generous supply of VWF A1 domain, and Dr P. J. Lenting for the gift of 418 mAb.

This work was supported by the Netherlands Organization for Scientific Research (NWO; grants 40-40100-98-05025 and 11-400-0076), the American Society of Hematology (W.B.), the National Heart, Lung, and Blood Institute (R01HL094594; W.B.), and an unrestricted grant from CSL Behring to S.E.M.S.

Authorship

Contribution: J.M.E.M.C, S.E.M.S., W.B., and J.W.M.H. designed the research; J.M.E.M.C., S.E.M.S., L.S., S.d.W., and M.A.H.F. performed experiments; K.H., H.D., and W.B. contributed research tools; all authors analyzed and interpreted data; and J.M.E.M.C., S.E.M.S., H.D., W.B., and J.W.M.H. wrote the manuscript.

Conflict-of-interest disclosure: This work was partly supported by an unrestricted grant from CSL Behring to S.E.M.S. The remaining authors declare no competing financial interests.

Correspondence: Johan W. M. Heemskerk, Department of Biochemistry (CARIM), Maastricht University, PO Box 616, 6200 MD Maastricht, The Netherlands; e-mail: jwm.heemskerk@bioch.unimaas.nl.

References

1. Mackman N, Tilley RE, Key NS. Role of the extrinsic pathway of blood coagulation in hemostasis and thrombosis. *Arterioscler Thromb Vasc Biol.* 2007;27(8):1687-1693.
2. Cho J, Furie BC, Coughlin SR, Furie B. A critical role for extracellular protein disulfide isomerase during thrombus formation in mice. *J Clin Invest.* 2008;118(3):1123-1131.
3. Gailani D, Renné T. The intrinsic pathway of coagulation: a target for treating thromboembolic disease? *J Thromb Haemost.* 2007;5(6):1106-1112.
4. van der Meijden PE, Schoenwaelder SM, Cosemans JMEM, et al. Dual P2Y12 receptor signaling in thrombin-stimulated platelets: involvement of phosphoinositide 3-kinase beta but not gamma isoforms in Ca2+ mobilization and procoagulant activity. *FEBS J.* 2008;275(2):371-385.
5. Heemskerk JWM, Kuijpers MJE, Munnix ICA, Siljander PRM. Platelet collagen receptors and coagulation. A characteristic platelet response as possible target for antithrombotic treatment. *Trends Cardiovasc Med.* 2005;15(3):86-92.

6. Monroe DM, Hoffman M. What does it take to make the perfect clot? *Arterioscler Thromb Vasc Biol.* 2006;26(1):41-48.
7. Dale GL. Coated-platelets: an emerging component of the procoagulant response. *J Thromb Haemost.* 2005;3(10):2185-2192.
8. Munnix ICA, Cosemans JMEM, Auger JM, Heemskerk JWM. Platelet response heterogeneity in thrombus formation. *Thromb Haemost.* 2009;102(6):1149-1156.
9. Reverter JC, Béguin S, Kessels H, Kumar R, Hemker HC, Coller BS. Inhibition of platelet-mediated, tissue-factor-induced thrombin generation by the mouse/human chimeric 7E3 antibody. Potential implications for the effect of c7E3 Fab treatment on acute thrombosis and 'clinical restenosis'. *J Clin Invest.* 1996;98(3):863-874.
10. Pedicord DL, Thomas BE, Mousa SA, Dicker IB. Glycoprotein IIb-IIIa receptor antagonists inhibit the development of platelet procoagulant activity. *Thromb Res.* 1998;90(6):247-258.
11. Ruggeri ZM. The role of von Willebrand factor in thrombus formation. *Thromb Res.* 2007; 120(suppl 1):S5-S9.
12. Lillicrap D. Von Willebrand disease: phenotype versus genotype, deficiency versus disease. *Thromb Res.* 2007;120(Suppl 1):S11-S16.
13. Béguin S, Kumar R, Keularts I, Seligsohn U, Coller BS, Hemker HC. Fibrin-dependent platelet procoagulant activity requires GpIb-V-IX receptors and von Willebrand factor. *Blood.* 1999;93(2): 564-570.
14. Keuren JFW, Ulrichts H, Feijge MAH, et al. Integrin alphaIIbbeta3 and shear-dependent action of glycoprotein Ibalpha stimulate platelet-dependent thrombin formation in stirred plasma. *J Lab Clin Med.* 2003;141(5):350-358.
15. Weiss HJ, Sussman II, Hoyer LW. Stabilization of factor VIII in plasma by the von Willebrand factor. Studies on posttransfusion and dissociated factor VIII and in patients with von Willebrand's disease. *J Clin Invest.* 1977;60(2):390-404.
16. Kawasaki T, Kaida T, Arnout J, Vermylen J, Hoylaerts MF. A new animal model of thrombophilia confirms that high plasma factor VIII levels are thrombogenic. *Thromb Haemost.* 1999;81(2): 306-311.
17. Weeterings C, De Groot PG, Adelmeijer J, Lisman T. The glycoprotein Ib-V-IX complex contributes to tissue factor-independent thrombin generation by recombinant factor VIIa on the activated platelet surface. *Blood.* 2008;112(8):3227-3233.
18. Dörmann D, Clemetson KJ, Kehrel B. The GpIb-V-IX thrombin-binding site is essential for thrombin-induced platelet procoagulant activity. *Blood.* 2000;96(7):2469-2478.
19. Hantgan RR, Hindriks G, Taylor RG, Sixma JJ, de Groot PG. Glycoprotein Ib, von Willebrand factor, and glycoprotein IIb-IIIa are all involved in platelet adhesion to fibrin in flowing whole blood. *Blood.* 1990;76(2):345-353.
20. Endenburg SC, Hantgan RR, Lindeboom-Blokzijl L, et al. On the role of von Willebrand factor in promoting platelet adhesion to fibrin in flowing blood. *Blood.* 1995;86(11):4158-4165.
21. Weeterings C, Adelmeijer J, Myles T, de Groot PG, Lisman T. Glycoprotein Ibalpha-mediated platelet adhesion and aggregation to immobilized thrombin under conditions of flow. *Arterioscler Thromb Vasc Biol.* 2006;26(3):670-675.
22. Huizinga EG, Tsuji S, Romijn RA, et al. Structures of glycoprotein Ibα and its complex with von Willebrand factor A1 domain. *Science.* 2002; 297(5584):1176-1179.
23. Cauwenberghs N, Ajzenberg N, Vauterin S, et al. Characterization of murine anti-glycoprotein Ib monoclonal antibodies that differentiate between shear-induced and ristocetin/botrocetin-induced glycoprotein Ib-von Willebrand factor interaction. *Haemostasis.* 2000;30(3):139-148.
24. Ulrichts H, Vanhoorelbeke K, Cauwenberghs S, et al. Von Willebrand factor but not alpha-thrombin binding to platelet glycoprotein Ibalpha is influenced by the HPA-2 polymorphism. *Arterioscler Thromb Vasc Biol.* 2003;23(7):1302-1307.
25. Keuren JFW, Wielders SJ, Ulrichts H, et al. Synergistic effect of thrombin on collagen-induced platelet procoagulant activity is mediated through protease-activated receptor-1. *Arterioscler Thromb Vasc Biol.* 2005;25(7):1499-1505.
26. Takahashi Y, Kalafatis M, Girma JP, Sewerin K, Andersson LO, Meyer D. Localization of a factor VIII binding domain on a 34 kilodalton fragment of the N-terminal portion of von Willebrand factor. *Blood.* 1987;70(5):1679-1682.
27. Ware J, Russell S, Ruggeri ZM. Generation and rescue of a murine model of platelet dysfunction: the Bernard-Soulier syndrome. *Proc Natl Acad Sci U S A.* 2000;97(6):2803-2808.
28. Denis C, Methia N, Frenette PS, et al. A mouse model of severe von Willebrand disease: defects in hemostasis and thrombosis. *Proc Natl Acad Sci U S A.* 1998;95(16):9524-9529.
29. Kinlough-Rathbone RL, Perry DW, Rand ML, Packham MA. Effects of cathepsin G pretreatment of platelets on their subsequent responses to aggregating agents. *Thromb Res.* 1999;95(6): 315-323.
30. Bergmeier W, Rackebrandt K, Schroder W, Zirngibl H, Nieswandt B. Structural and functional characterization of the mouse von Willebrand factor receptor GpIb-V-IX/IX with novel monoclonal antibodies. *Blood.* 2000;95(3):886-893.
31. Stefanini L, Roden RC, Bergmeier W. CalDAG-GEFI is at the nexus of calcium-dependent platelet activation. *Blood.* 2009; 114(12):2506-2514.
32. Munnix ICA, Strehl A, Kuijpers MJE, et al. The glycoprotein VI-phospholipase Cgamma2 signaling pathway controls thrombus formation induced by collagen and tissue factor in vitro and in vivo. *Arterioscler Thromb Vasc Biol.* 2005;25(12):2673-2678.
33. Vanschoonbeek K, Wouters K, van der Meijden PEJ, et al. Anticoagulant effect of dietary fish oil in hyperlipidemia: an mRNA expression study in APOE2 knock-in mice. *Arterioscler Thromb Vasc Biol.* 2008;28(11):2023-2029.
34. Munnix ICA, Kuijpers MJE, Auger JM, et al. Segregation of platelet aggregatory and procoagulant microdomains in thrombus formation: regulation by transient integrin activation. *Arterioscler Thromb Vasc Biol.* 2007;27(11):2484-2490.
35. Vanschoonbeek K, Feijge MAH, van Kampen RJW, et al. Initiating and potentiating roles of platelets in tissue factor-induced thrombin generation in the presence of plasma: subject-dependent variation in thrombogram characteristics. *J Thromb Haemost.* 2004;2(3):476-484.
36. Kulkarni S, Jackson SP. Platelet factor XIII and calpain negatively regulate integrin alphaIIbbeta3 adhesive function and thrombus growth. *J Biol Chem.* 2004;279(29):30697-30706.
37. Pidard D, Renesto P, Berndt MC, Rahbi S, Clemetson KJ, Chignard M. Neutrophil proteinase cathepsin G is proteolytically active on the human platelet glycoprotein Ib/IX receptor, characterization of the cleavage site within the glycoprotein Ibα subunit. *Biochem J.* 1994;303(Pt 2): 489-498.
38. Renesto P, Si-Tahar M, Moniatte M, et al. Specific inhibition of thrombin-induced activation by the neutrophil proteinases elastase, cathepsin G, and proteinase 3: evidence for distinct cleavage sites within the aminoterminal domain of the thrombin receptor. *Blood.* 1997;89(6):1944-1953.
39. Sambrano GR, Huang W, Faruqi T, Mahrus S, Craik C, Coughlin SR. Cathepsin G activates protease-activated receptor-4 in human platelets. *J Biol Chem.* 2000;275(10):6819-6823.
40. Bergmeier W, Bouvard D, Eble JA, et al. Rhodocytin (aggretin) activates platelets lacking alpha2beta1 integrin, glycoprotein VI, and the ligand-binding domain of glycoprotein Ibalpha. *J Biol Chem.* 2001;276(27):25121-25126.
41. Keuren JF, Baruch D, Legendre P, et al. von Willebrand factor C1C2 domain is involved in platelet adhesion to polymerized fibrin at high shear rate. *Blood.* 2004;103(5):1741-1746.
42. Parker RI, Gralnick HR. Fibrin monomer induces binding of endogenous platelet von Willebrand factor to the glycocalicin portion of platelet glycoprotein Ib. *Blood.* 1987;70(5):1589-1594.
43. Vanhoorelbeke K, Ulrichts H, Van de Walle G, Fontayne A, Deckmyn H. Inhibition of platelet glycoprotein Ib and its antithrombotic potential. *Curr Pharm Des.* 2007;13(26):2684-2697.
44. Ruggeri ZM, Dent JA, Saldívar E. Contribution of distinct adhesive interactions to platelet aggregation in flowing blood. *Blood.* 1999;94(1):172-178.
45. Chauhan AK, Kisucka J, Lamb CB, Bergmeier W, Wagner DD. von Willebrand factor and factor VIII are independently required to form stable occlusive thrombi in injured veins. *Blood.* 2007;109(6): 2424-2429.
46. Bergmeier W, Chauhan AK, Wagner DD. Glycoprotein Ibalpha and von Willebrand factor in primary platelet adhesion and thrombus formation: lessons from mice. *Thromb Haemost.* 2008;99(2): 264-270.
47. Müller F, Mutch NJ, Schenk WA, et al. Platelet polyphosphates are proinflammatory and procoagulant mediators in vivo. *Cell.* 2009;139(6): 1143-1156.
48. Watson SP, Auger JM, McCarty OJ, Pearce AC. GPVI and integrin alphaIIbbeta3 signaling in platelets. *J Thromb Haemost.* 2005;3(8):1752-1762.